

B. Mohammadi · K. Krampfl · C. Cetinkaya
H. Moschref · J. Grosskreutz · R. Dengler · J. Bufler

Kinetic analysis of recombinant mammalian α_1 and $\alpha_1\beta$ glycine receptor channels

Received: 18 October 2002 / Accepted: 20 January 2003 / Published online: 19 February 2003
© EBSA 2003

Abstract To analyze the influence of the β -subunit on the kinetic properties of GlyR channel currents, α_1 -subunits and $\alpha_1\beta$ -subunits were transiently expressed in HEK 293 cells. A piezo dimorph was used for fast application of glycine to outside-out patches. The rise time of activation was dose dependent for both receptors and decreased with increasing glycine concentrations. Subunit composition had no effect on the time course of activation. Coexpression of α_1 - and β -subunits resulted in a significantly lower EC_{50} and a reduced slope of the dose–response curve of glycine compared with expression of α_1 -subunits alone. For both receptor subtypes, the time course of desensitization was concentration dependent. Desensitization was best fitted with a single time constant at 10–30 μ M, with two at 0.1 mM, and at saturating concentrations (0.3–3 mM) with three time constants. Desensitization of homomeric α_1 -receptor channels was significantly slower than that of $\alpha_1\beta$ -receptor channels. The time course of current decay after the end of glycine pulses was tested at different pulse durations of 1 mM glycine. It was best fitted with two time constants for both α_1 and $\alpha_1\beta$ GlyR channels, and increased significantly with increasing pulse duration.

Keywords Recombinant glycine receptors · Desensitization · Deactivation · Resensitization · Fast application

Introduction

The strychnine-sensitive glycine receptor (GlyR) channel is a member of an ion channel superfamily which includes nicotinic acetylcholine, GABA_A and serotonin (5-HT₃) receptor channels (Unwin 1989; Betz 1990). The highest density of expression has been found in the brain stem and spinal cord (Langosch et al. 1990). GlyR channels have been purified from mammalian spinal cord (Graham et al. 1985). They form pentamers composed of the ligand-binding α -subunits and optionally an additional β -subunit (Langosch et al. 1990). The α -subunit exists in various isoforms (α_1 – α_4), whereas only one form of the β -subunit is known (Betz et al. 1991). High levels of α_1 -transcripts are found mainly in the spinal cord and the brain stem (Betz et al. 1991). During development, α_2 -receptor isoforms are largely replaced by adult receptors consisting of the α_1 - and β -subunits (Becker et al. 1988; Malosio et al. 1991; Watanabe and Akagi 1995). α_3 -subunits occur at low levels in the olfactory bulb, cerebellum and spinal cord. Low levels of α_4 -subunits were found in the adult mouse brain (Malosio et al. 1991). In contrast to the β -subunit, α -subunits form functional homomeric receptor channels (Schmieden et al. 1989; Grenningloh et al. 1990; Kuhse et al. 1990, 1991; Handford et al. 1996). The β -subunit is distributed in many regions of the rat central nervous system (Malosio et al. 1991).

After binding of glycine to GlyR channels, an integrated ion channel pore opens which is selectively permeable for chloride. The transient increase in the chloride permeability shifts the transmembrane potential toward the chloride equilibrium potential (Kandel et al. 1995). The biophysical properties of GlyR channels have been studied on native receptors from zebra-fish larvae (Legendre 1998), guinea-pig ventral cochlear nucleus neurons (Harty and Manis 1998) and rat motoneurons (Singer and Berger 1999) using methods of ultrafast agonist application in the submillisecond range. One study dealing with the biophysical properties of

B. Mohammadi · K. Krampfl · C. Cetinkaya · H. Moschref
J. Grosskreutz · R. Dengler · J. Bufler (✉)
Department of Neurology,
Medical School University Hannover,
Carl-Neuberg-Str. 1, 30625 Hannover, Germany
E-mail: Bufler.Johannes@MH-Hannover.de
Tel.: +49-511-5322439
Fax: +49-511-5323115

recombinant homomeric α_1 -GlyR channels used laser-pulse photolysis in combination with a U-tube system for solution exchange (Greuer 1999). Single-channel analysis of GlyR channels revealed four subconductance levels (Bormann et al. 1993; Legendre 1997; Rajendra et al. 1995). To our knowledge, one study exists dealing with biophysical properties of recombinant homomeric α_1 -GlyR channels using laser-pulse photolysis in combination with a U-tube system for solution exchange (Greuer 1999). In the present study, we were interested in two topics: (1) the biophysical analysis of the activation, desensitization, deactivation, and resensitisation characteristics of recombinant homomeric α_1 -GlyR channels, and (2) the influence of cotransfected β -subunits on the kinetics of recombinant GlyR channels.

Materials and methods

Transformed human embryonic kidney (HEK) 293 cells were cultured in Dulbecco's modified Eagle's medium (DMEM) supplemented with 10% fetal calf serum (FCS), 100 U/ml penicillin, and 100 μ g/ml streptomycin at 37°C in a 5% CO₂/95% air incubator. They were plated on 12-mm glass coverslips coated with poly-L-lysine. Cells were suspended in a buffer used for transfection containing: 50 mM K₂HPO₄ and 20 mM K-acetate at pH 7.35. cDNAs of human α_1 -GlyR or human α_1 -GlyR with rat β -GlyR subunits (subcloned in pCIS2 expression vector) were added to the suspended cells (25 μ g/ml cDNA for each subunit). A reporter cDNA encoding green fluorescent protein (GFP, 10 μ g/ml) was used to visually identify transfected cells. Transfection was performed using an electroporation device (EquiBio, UK) as recently described (Mohammadi et al. 2001). Transfected cells were replated on glass cover slips in DMEM containing 10% FCS and incubated for 15–24 h prior to the experiments. The transfection rate was 10–20%, as seen by the proportion of cells marked by GFP-fluorescence. Media and FCS were obtained from Biochrom (Berlin, Germany) and chemicals from Sigma (St Louis, USA).

Patch-clamp experiments were performed on outside-out patches containing glycine receptors at room temperature, using standard methods (Hamill et al. 1981). Cells were bathed in extracellular solution containing (in mM): 162 NaCl, 5.3 KCl, 2.0 CaCl₂, 0.6 Na₂HPO₄, 0.22 KH₂PO₄, 15 HEPES, and 5.6 glucose at pH 7.4. Patch pipettes were pulled from borosilicate glass tubes with filament (Clark, Pangbourne, UK) using a DMZ-puller (Zeitz Instruments, Augsburg, Germany) and filled with a solution containing (in mM): 140 KCl, 2 MgCl₂, 11 EGTA, 10 HEPES, and 10 glucose. Outside-out patches were obtained using standard methods. Currents were recorded with an EPC9 patch-clamp amplifier (List Instruments, Darmstadt, Germany). Data were sampled at 20 kHz on a hard disk, low-pass filtered at 5 kHz and analyzed with pCLAMP software (Axon Instruments, Foster City, CA, USA).

Glycine-containing test solutions were applied using a piezobimorph (Franke et al. 1987). The time for solution exchange with an outside-out patch in place was < 100 μ s (Bufler et al. 1996; Jahn et al. 1998; Krampfl et al. 2002a, 2002b), and at best ~40 μ s. It was therefore at least three times faster than the fastest current response onset observed after the application of a saturating glycine concentration (Fig. 2a). Between three and eight single current traces were averaged for analysis. To determine the time course of current decay (desensitization and deactivation, Figs. 3, 4), the number of time constants of current decay was increased until addition of a further exponential did not significantly improve the quality of the fit (Haas and Macdonald 1999). Experimental data are given as mean \pm SEM. All parameters of the α_1 -GlyR and $\alpha_1\beta$ -GlyR channels determined in the study [rise time (Fig. 2a), EC₅₀ (Fig. 2b),

desensitization (Fig. 3), deactivation (Fig. 4)] were statistically tested with the independent Student *t*-test. The respective *p* values are indicated in the Results section. The experimental data were assumed not to differ significantly when the respective *p* values were > 0.05. The experimental values in the results section are given first for the α_1 -homomeric GlyR channels, and secondly for $\alpha_1\beta$ -GlyR channels.

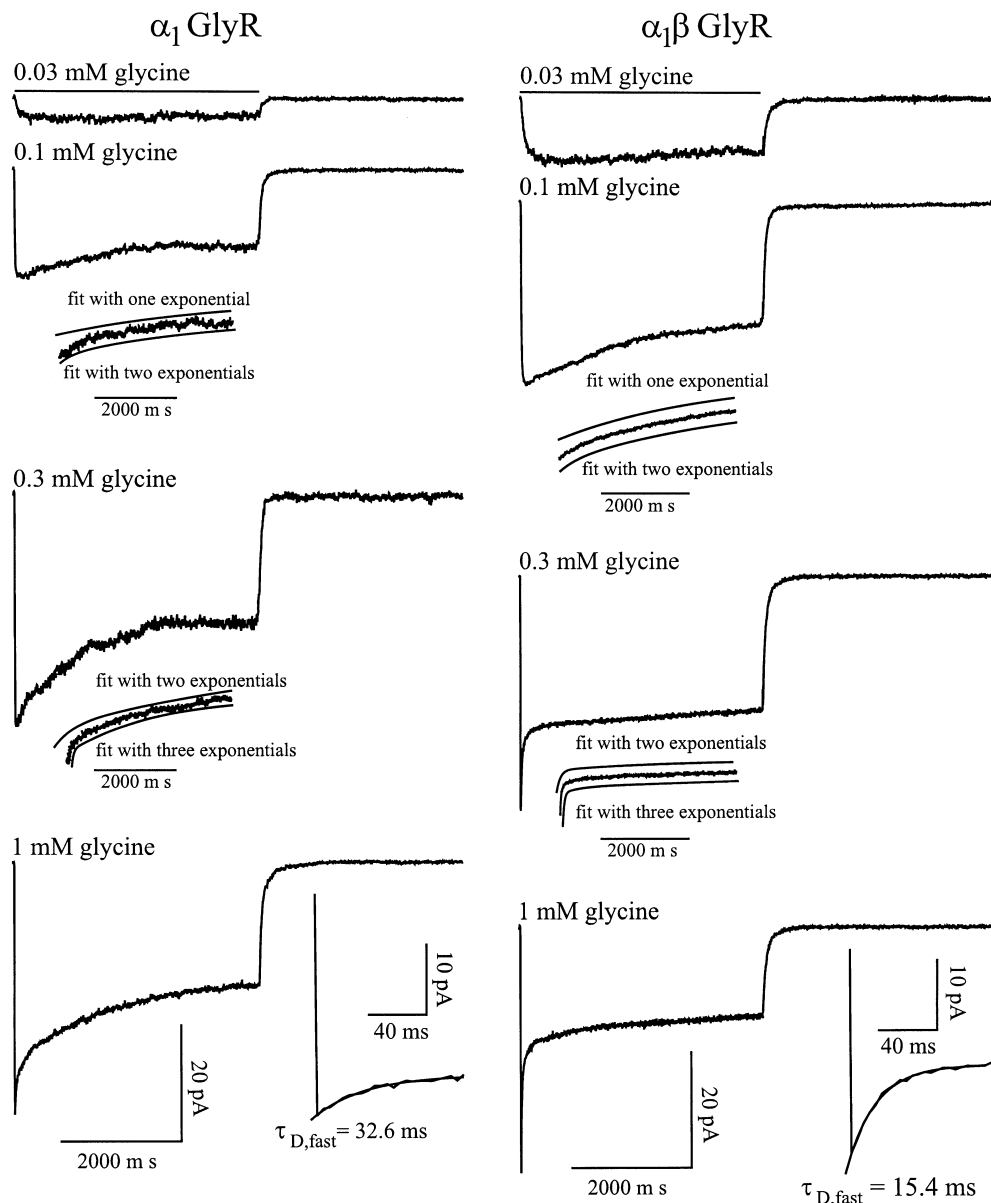
Results

Examples of currents obtained from outside-out patches in response to 4 s pulses of different glycine concentrations to α_1 -GlyR and $\alpha_1\beta$ -GlyR channels are shown in Fig. 1. In these experiments, the 10–90% rise time of α_1 -GlyR and $\alpha_1\beta$ -GlyR channels decreased from 72.2 ms and 73.4 ms at 0.03 mM glycine to 0.35 ms and 0.32 ms at 1 mM glycine, respectively. The peak current amplitude reached its maximum at 1 mM glycine. In the presence of the agonist, the current decayed dependent on concentration due to desensitization by around 40% at higher glycine concentrations. At 0.03 mM glycine, both receptors desensitized slowly, best fitted with a single exponential ($\tau_{D,slow}$ was 3,125 ms and 1,876 ms in this experiment). A second, faster desensitizing component was observed at 0.1 mM glycine ($\tau_{D,intermediate}$ was 454 ms and 265 ms). When ≥ 0.3 mM glycine was applied, desensitization became triexponential (at 0.3 mM glycine, $\tau_{D,fast}$ was 40 ms and 24 ms; at 1 mM glycine 33 ms and 15 ms). The insets in Fig. 1 show the fits of desensitization with one, two, or three exponentials at application of 0.1 and 0.3 mM glycine at both receptor types. The insets at the bottom of Fig. 1 show the fast component of desensitization at 1 mM glycine on an expanded time scale.

In Fig. 2, the rise time and dose–response curve of α_1 -GlyR and $\alpha_1\beta$ -GlyR channel currents after application of 4 s pulses of different glycine concentrations is further analyzed. The rise time (Fig. 2a) decreased with higher glycine concentrations and was 193 ± 22 ms and 185 ± 29 ms at 0.01 mM glycine, and 0.37 ± 0.07 ms and 0.34 ± 0.05 ms at 1 mM glycine (see insets, no significant difference). To construct dose–response diagrams, the peak current amplitude at each glycine concentration was normalized to the peak current amplitude at 1 mM glycine (Fig. 2b). The relative peak current amplitude increased with increasing concentrations of glycine (Fig. 2b). The dose–response curve of α_1 -GlyR channels (straight line) was shifted towards higher glycine concentrations ($p < 0.001$) with an EC₅₀ of 105 μ M compared with 61 μ M of $\alpha_1\beta$ -GlyR channels (dashed line) (Fig. 2). The slope of the dose–response curve (calculated by the Hill equation) was steeper for α_1 -GlyR (2.2 ± 0.5 , $n = 6$) than for $\alpha_1\beta$ -GlyR channels (1.6 ± 0.1 , $n = 6$) corresponding to previously published data (Laube et al. 2000; Bormann et al. 1993; Handford et al. 1996).

The currents in Fig. 1 show the complex desensitization pattern of GlyR channels. Desensitization could be fitted with one, two, or three exponentials dependent on

Fig. 1 Glycine-activated currents of outside-out patches containing recombinant GlyR channels. Currents of homomeric α_1 -GlyR (left-hand side) or heteromeric $\alpha_1\beta$ -GlyR channels (right-hand side) recombinantly expressed in HEK 293 cells were shown in response to 4 s pulses of different concentrations of glycine (0.03–1 mM). The holding potential was -40 mV in both experiments. The insets of the currents elicited at 0.1 and 0.3 mM glycine show the fit of desensitization with two or three exponentials. The insets of the currents elicited at 1.0 mM glycine show the fast component of desensitization at 1 mM glycine with an expanded time scale



the glycine concentration. It was further analyzed in Fig. 3. $\tau_{D,slow}$ decreased significantly ($p < 0.001$) from $3,319 \pm 271$ ms ($n = 5$) and $1,889 \pm 163$ ms ($n = 5$) at 0.03 mM glycine to $1,537 \pm 199$ ms ($n = 5$) and 512 ± 31 ms ($n = 5$) at 3 mM glycine ($p < 0.001$) (Fig. 3a). It was significantly slower at α_1 -GlyR channels at all glycine concentrations ($p < 0.001$). The relative proportion of $\tau_{D,slow}$ on the whole current amplitude increased slightly from $5.9 \pm 1.7\%$ ($n = 5$) and $8.0 \pm 1.8\%$ ($n = 5$) at 0.03 mM to $13.2 \pm 2.5\%$ ($n = 5$) and $11.0 \pm 3.6\%$ ($n = 5$) at 3 mM glycine (Fig. 3b). There was no significant difference between α_1 -GlyR and $\alpha_1\beta$ -GlyR channels at all glycine concentrations. At glycine concentrations ≥ 0.1 mM, a faster component of desensitization, $\tau_{D,intermediate}$, appeared (Fig. 3c). $\tau_{D,intermediate}$ decreased significantly from 480 ± 69 ms ($n = 5$) and 288 ± 74 ms ($n = 5$) at 0.1 mM glycine to 312 ± 17 ms ($n = 5$) and 137 ± 12 ms ($n = 5$) at 3 mM ($p < 0.005$). The relative proportion of

$\tau_{D,intermediate}$ on the whole current amplitude increased from $5.9 \pm 2.2\%$ ($n = 5$) and $10.0 \pm 5.1\%$ ($n = 5$) at 0.1 mM to $19.2 \pm 5.4\%$ ($n = 5$) and $14.5 \pm 2.4\%$ ($n = 5$) at 3 mM glycine (Fig. 3d). There was no significant difference between α_1 -GlyR and $\alpha_1\beta$ -GlyR channels at all glycine concentrations. A third, fast component of desensitization, $\tau_{D,fast}$, was found at glycine concentrations ≥ 0.3 mM (Fig. 3e). $\tau_{D,fast}$ decreased significantly ($p < 0.001$) from 38.7 ± 5.1 ms ($n = 5$) and 22.6 ± 2.3 ms ($n = 5$) at 0.3 mM to 29.1 ± 4.3 ms ($n = 5$) and 12.2 ± 1.4 ms ($n = 5$) when 3 mM glycine was applied. The relative proportion of $\tau_{D,fast}$ on the whole current amplitude increased from $14.8 \pm 1.7\%$ and $23.0 \pm 5.6\%$ at 0.3 mM to $22.0 \pm 2.7\%$ and $42.6 \pm 7.10\%$ at 3 mM glycine (Fig. 3f). This effect was significantly more pronounced at $\alpha_1\beta$ -GlyR channels at glycine concentrations ≥ 1.0 mM ($p < 0.001$). The relative steady-state current amplitude decreased from $94.1 \pm 1.7\%$ ($n = 5$) and

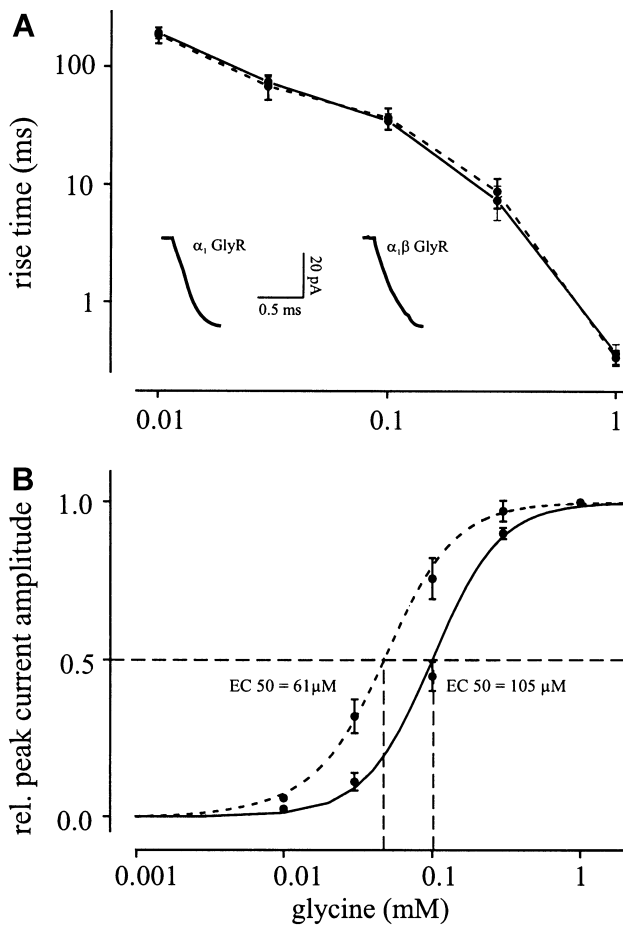


Fig. 2a, b Dose–response relationship of the rise time and peak current amplitude of glycine-activated currents. The straight line shows data of α_1 -GlyR and the dashed line of $\alpha_1\beta$ -GlyR channels. Glycine was applied in concentrations between 0.3 and 3 mM glycine. **a** 10–90% rise time of glycine-activated currents was plotted vs glycine concentration (mM) in a double logarithmic plot (no statistical difference). The insets show the onset of the current of both receptors after application of 1 mM glycine at an extended time scale. **b** The normalized peak current amplitude was plotted vs the glycine concentration (mM) in a semilogarithmic plot. Each point in the diagrams represents data from at least five experiments

$92.0 \pm 1.8\%$ ($n = 5$) at 0.03 mM to $45.5 \pm 4.0\%$ ($n = 5$) and $32.4 \pm 3.3\%$ ($n = 5$) at 3 mM glycine (Fig. 3g). It was lower at $\alpha_1\beta$ -GlyR channels at glycine concentrations ≥ 0.1 mM ($p < 0.01$).

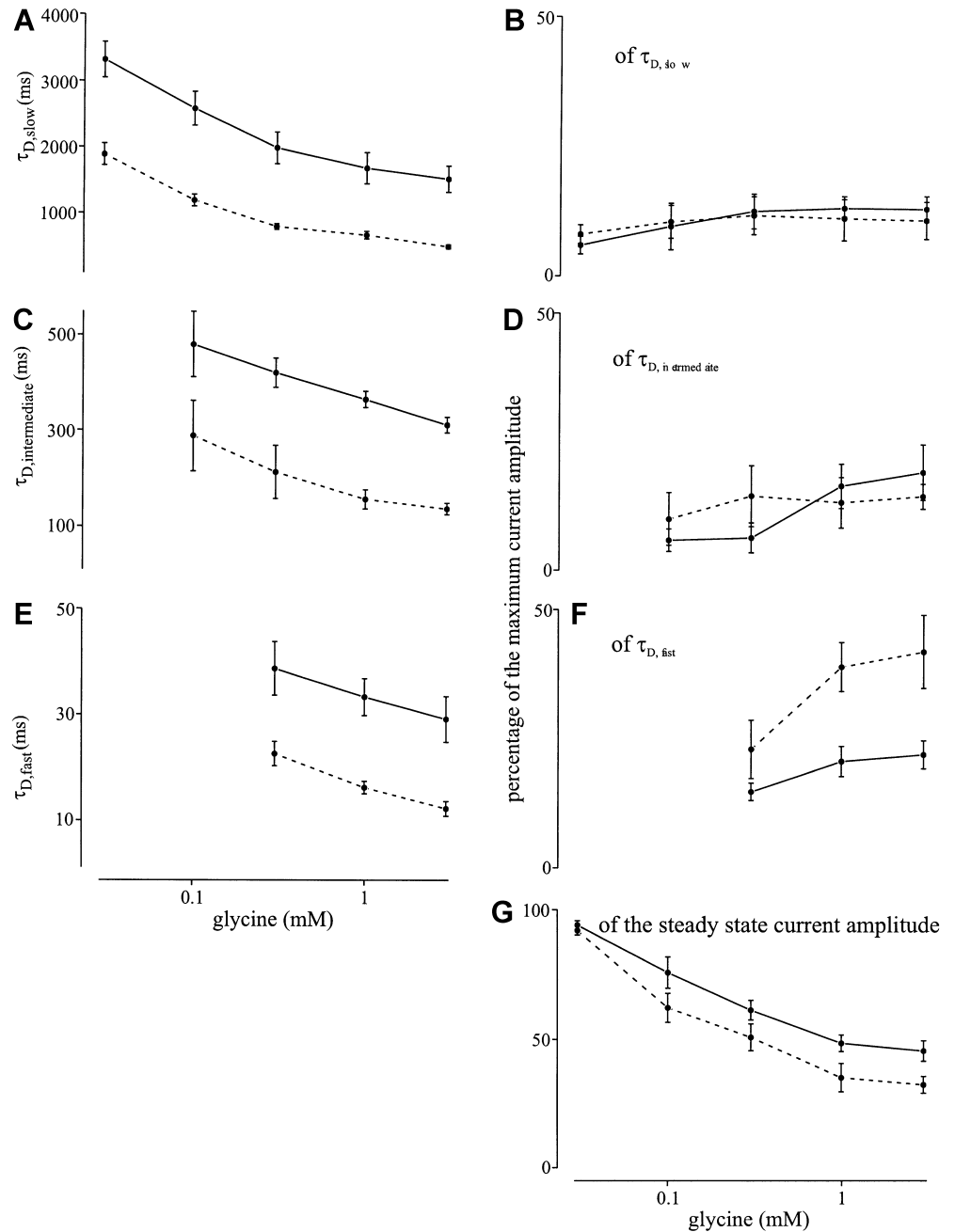
Under physiological conditions, the transmitter is present in the synaptic cleft only for a short time (about 1–2 ms), resulting in the fast decay of inhibitory postsynaptic potentials (Legendre 1998). The time course of current decay after the end of agonist pulses, deactivation, is determined by the unbinding rate of glycine from the receptor, the isomerization rate constants, and the time constants of desensitization. In Fig. 4a and b, application of 2, 200 and 2,000 ms pulses of 1 mM glycine to α_1 -GlyR and $\alpha_1\beta$ -GlyR channels is shown. On the right-hand side, the current decay after the end of the respective glycine pulse was scaled up to the same time axis and amplitude. Deactivation was

fitted with two exponentials ($\tau_{\text{deact,fast}}$, $\tau_{\text{deact,slow}}$) showing slower time constants at longer pulse duration. $\tau_{\text{deact,fast}}$ for α_1 -channels and $\alpha_1\beta$ -channels increased from 5.5 ± 0.4 ms ($n = 5$) and 6.5 ± 0.9 ms ($n = 5$) after 2 ms to 18.3 ± 3.1 ms ($n = 5$) and 19.1 ± 2.7 ms ($n = 5$) after 200 ms pulses (Fig. 4c, left diagram, no statistical significance between both receptors), and $\tau_{\text{deact,slow}}$ rose from 20.6 ± 3.9 ms ($n = 5$) and 33.8 ± 6.4 ms ($n = 5$) after 2 ms to 115.5 ± 7.2 ms ($n = 7$) and 137.3 ± 11.8 ms ($n = 5$) after 2000 ms pulses of 1 mM glycine (Fig. 4c, right diagram). $\tau_{\text{deact,slow}}$ had a tendency towards slower values at $\alpha_1\beta$ -GlyR channels.

The standard deviation of deactivation from mono- or biexponential fits was tested for statistical significance. The biexponential fit of the time course of deactivation was significantly better for both receptors ($p < 0.05$) when short glycine pulses were applied. At 2,000 ms glycine pulses, however, biexponential fitting did not increase the quality of the fit (Fig. 5). The time constant of deactivation, τ_{deact} , was 93.2 ms (mean 90.3 ± 15.1 ms, $n = 5$) and 101.8 ms (mean 114.4 ± 16.1 ms, $n = 4$) for α_1 -GlyR and $\alpha_1\beta$ -GlyR channels (Fig. 4a, b).

To analyze the time course of the recovery from desensitization, double-pulse experiments were performed. Figure 6 shows the repetitive application of 1 mM glycine to α_1 -GlyR (Fig. 6a) and $\alpha_1\beta$ -GlyR channels (Fig. 6b). As discussed in Figs. 1 and 3, GlyR channel currents desensitized with different time constants to a steady-state amplitude at both receptors. When it is assumed that different time constants of desensitization represent the transition from one or more open states to different desensitized states of the receptor (see Figs. 1 and 3), it can be hypothesized that the time course of recovery from different desensitized states depends on different rate constants. To test this hypothesis, we performed double pulse experiments with increasing intervals between 1 mM glycine pulses and a duration of the first pulse of 200 ms (Fig. 6, upper traces) and 4000 ms (Fig. 6, lower traces) followed by a second 20 ms pulse to α_1 -GlyR (Fig. 6a) and $\alpha_1\beta$ -GlyR channels (Fig. 6b). When the second pulse was applied immediately after complete deactivation of the currents, the peak current amplitude of the second 1 mM glycine pulse was equal to that at the end of the preceding pulse (Fig. 6). With increasing intervals between pulses, the peak current amplitude of the second pulse increased and approximated that of the first pulse. The time course of resensitization could be fitted monoexponentially at α_1 -GlyR and $\alpha_1\beta$ -GlyR channels and it increased with increasing duration of the first pulse (see the straight curves in Fig. 6). The time constants of resensitization, τ_{rec} , after 200 ms pulses (upper panel) were 389 ms (mean 481 ± 208 ms, $n = 4$) and 358 ms (mean 521 ± 298 ms, $n = 4$), and after 4,000 ms pulses (lower panel), the values of τ_{rec} were 2,197 ms (mean $2,062 \pm 592$ ms, $n = 4$) and 1,599 ms (mean $1,412 \pm 409$ ms, $n = 4$) for α_1 -GlyR and $\alpha_1\beta$ -GlyR channels, respectively. There was no statistically significant difference of τ_{rec} between both receptors, but the decrease of τ_{rec} with increasing

Fig. 3 Dose–response relationship of the time constants of desensitization of glycine-activated currents. The *straight line* shows data from α_1 -GlyR channels and the *dashed line* from $\alpha_1\beta$ -GlyR channels. Time constants of desensitization and their relative proportion on the whole current amplitude are plotted vs glycine concentration: **a** concentration dependence of $\tau_{D,slow}$; **b** the relative proportion of $\tau_{D,slow}$ on the whole current amplitude; **c** concentration dependence of $\tau_{D,intermediate}$; **d** the relative proportion of $\tau_{D,intermediate}$ on the whole current amplitude; **e** concentration dependence of $\tau_{D,fast}$; **f** the relative proportion of $\tau_{D,fast}$ on the whole current amplitude. It was more pronounced at $\alpha_1\beta$ -GlyR channels at glycine concentrations ≥ 1.0 mM ($p < 0.001$); **g** dose–response relationship of the relative proportion of the steady-state current on the whole current amplitude. Each point in the diagrams represents data from at least five experiments



duration of the first pulse from 200 ms to 4,000 ms was significant in both receptors ($p < 0.001$).

Discussion

GlyR channels are expressed with highest density in the brain stem and spinal cord (Langosch et al. 1990). They form pentamers composed of the ligand-binding α -subunits and optionally an additional β -subunit (Langosch et al. 1990). The α -subunit occurs in four isoforms, whereas only one isoform is known from the β -subunit (Betz et al. 1991). On the single channel level, it was shown that recombinant GlyR channels have different conductance levels and that coexpression of β -subunits

with different α -subunits results in the expression of channels with predominantly low conductance levels (Bormann et al. 1993). The present study is the first to analyze the kinetics of recombinant GlyR channels using techniques of ultrafast solution exchange to determine kinetic parameters dependent on the subunit composition of GlyR.

The time course of activation was identical at α_1 - and $\alpha_1\beta$ -receptor channels (Fig. 2a) and corresponded to that found in hindbrain neurons of zebra-fish larvae after application of a saturating glycine concentration (Legendre 1998). In contrast, native glycine receptors of the ventral cochlear nucleus of guinea pigs had a slower rise time at 1 mM glycine (Harty and Manis 1998), but this may be because of the slower speed of solution ex-

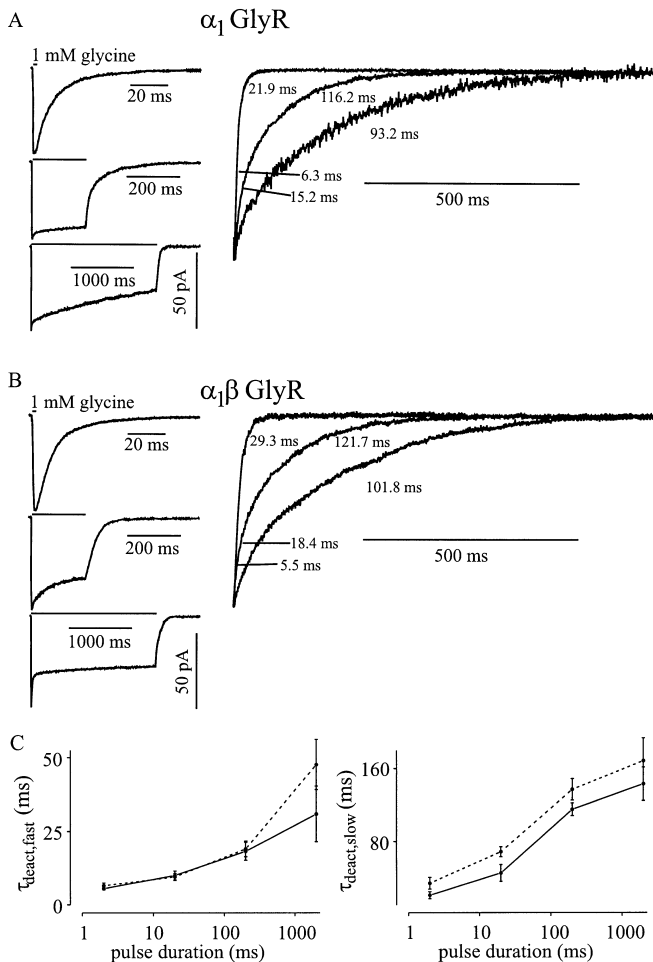


Fig. 4 Time course of deactivation after 1 mM glycine pulses. **a** 2 ms (upper trace), 200 ms (middle trace) and 2000 ms pulses (lower trace) of 1 mM glycine applied to outside-out patches containing α_1 -GlyR channels. *Left*, current traces shown at different time scales; *right*, current decay after the end of glycine pulses scaled up to the same time and amplitude. **b** Same experiment with $\alpha_1\beta$ -GlyR channels as shown in **a**. **c** Dependence of the time course of deactivation of $\tau_{\text{deact,fast}}$ (left) and $\tau_{\text{deact,slow}}$ (right) of α_1 -GlyR (straight line) and $\alpha_1\beta$ -GlyR channels (dashed line) on the pulse duration. Each point in the diagrams averages at least five experiments. Holding potential -40 mV in both experiments

change of the application system used in that study. The dose–response curve of GlyR was shifted to the left when both, α_1 - and β -subunits were expressed (Fig. 2b), but the slope of the dose–response curve was steeper at homomeric α_1 -GlyR channel currents. Higher sensitivity and lower Hill coefficients of $\alpha_1\beta$ -GlyR (EC_{50} : 48–187 μM ; Hill coefficient: 1.8–2.5) compared with α_1 -GlyR channels (EC_{50} : 18–260 μM ; Hill coefficient: 2.5–4.5) have also been reported in previous studies using different techniques (Schmieden et al. 1992; Bormann et al. 1993; Handford et al. 1996; Lewis et al. 1998; Laube et al. 2000). The slow components of desensitization as well as the steady-state current amplitude could be reliably determined with long 4 s glycine pulses. At low glycine

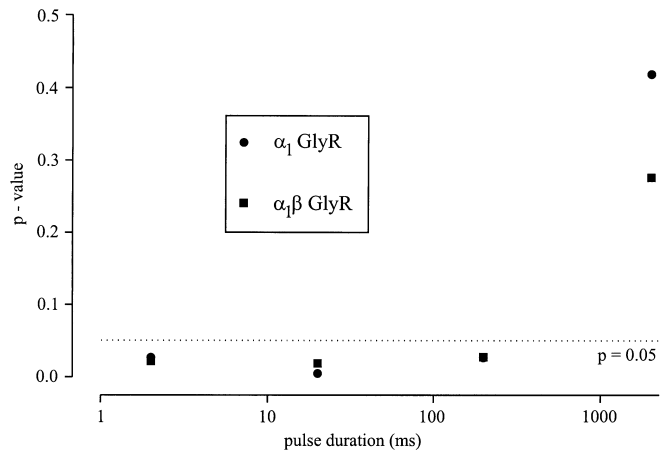


Fig. 5 Quality of monoexponential vs biexponential fits of the time course of deactivation of α_1 -GlyR and $\alpha_1\beta$ -GlyR channel currents, tested by Student's *t*-test for comparison of the standard deviation of the respective fits. The current decay after the end of pulses of 1 mM glycine was analyzed. Fits were tested by Student's *t*-test for independent samples for comparison of least square values of the respective fits. At 2,000 ms glycine pulses (1 mM), the biexponential fit did not surpass the monoexponential fit significantly ($p > 0.2$)

concentrations (0.03 mM), desensitization ($\tau_{\text{D,slow}}$) was monoexponential, at 0.1 mM glycine, desensitization became biphasic ($\tau_{\text{D,slow}}$ and $\tau_{\text{D,intermediate}}$) and, at saturating concentrations (0.3–3 mM glycine), a third component of desensitization emerged ($\tau_{\text{D,fast}}$) similar to the desensitization kinetics found at recombinant rat GABA_A receptor channels (Haas and Macdonald 1999; Krampfl et al. 2000). Homomeric α_1 -GlyR channels desensitized significantly more slowly at every glycine concentration (Figs. 1, 3a). The time constants of desensitization found in the study of Harty and Manis (1998) corresponded quite well to the desensitization kinetics found for $\alpha_1\beta$ -GlyR channels in our study. In contrast, desensitization of GlyR channels from hind-brain neurons of zebra-fish larvae was calculated with two time constants at saturating glycine concentrations (Legendre 1998). Similar to previous studies on GlyR -channel currents of ventral cochlear nucleus neurons (Harty and Manis 1998) and of hindbrain neurons of zebra-fish larvae (Legendre 1998), deactivation had a biexponential time course at recombinant GlyR channels. However, when 2-s pulses of glycine were applied, the time course of deactivation became monophasic (Fig. 5). Resensitization could be fitted with a single exponential (Fig. 6). In contrast to the desensitization and deactivation kinetics, resensitization was not affected by coexpression of the β -subunit.

Summarizing the experimental results, the analysis of macroscopic currents revealed that $\alpha_1\beta$ -GlyR channels had a higher affinity for glycine with a lower slope of the dose–response curve (Fig. 2b) and faster desensitization kinetics (Fig. 3). Another main finding which was not previously reported is that the time course of deactivation and resensitization depended on the pulse

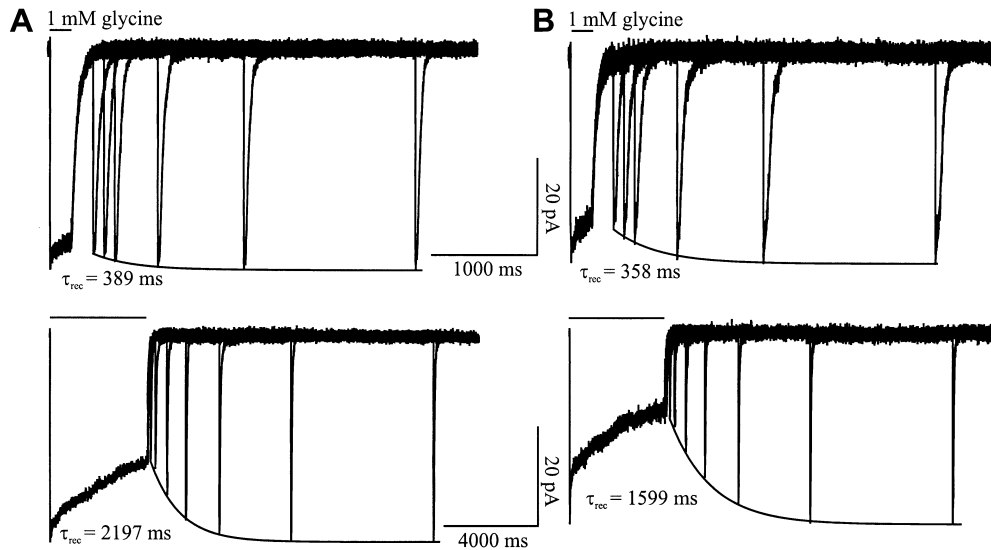


Fig. 6 The time course of recovery from desensitization of α_1 -GlyR (a) and $\alpha_1\beta$ -GlyR (b) channels. Double-pulse experiments were performed with increasing intervals between 1 mM glycine pulses. The first pulse had a duration of 200 ms (*upper traces*) or 4,000 ms (*lower traces*) followed by a second 20 ms pulse. The time constant of resensitization (τ_{rec}) could be determined with a monoexponential fit for both channels. There was no statistical significant difference of τ_{rec} between both receptors, but the decrease of τ_{rec} with increasing duration of the first pulse from 200 ms to 4,000 ms was significant in both receptors ($p < 0.001$)

duration at both receptors (Fig. 4, 6), but there was no significant difference between α_1 -GlyR and $\alpha_1\beta$ -GlyR channels. Kinetic differences between the studies of Harty and Manis (1998) and Singer and Berger (1999) performed on GlyR-channels of ventral cochlear nucleus neurons and motoneurons may arise from molecular differences in the native GlyR-channels used in these studies.

Some points crucial for the interpretation of the kinetics of recombinant GlyR channels and for the functional role of the β -subunit arise from our data: 1. The higher affinity for glycine and the lower slope of the dose–response curve of $\alpha_1\beta$ -GlyR channel currents predict different values of the binding and unbinding rate constants of glycine at the receptor compared with homomeric α_1 -GlyR channels. 2. The faster desensitization and lower steady-state current amplitude of $\alpha_1\beta$ -GlyR compared with α_1 -GlyR channels point, under equilibrium conditions, to faster isomerization from one or more open states of the channels (Twyman and Macdonald 1991) to different desensitized states in the presence of the β -subunit. 3. Deactivation measures the time course of unbinding of an agonist from the receptor and parallels the single channel burst duration under specific conditions (Jahn et al. 2001; Krampfl et al. 2002b; Wyllie et al. 1998). GlyR channels have different open states with distinct single channel slope conductance and burst duration, as revealed by single channel analysis (Bormann et al. 1993; Laube et al. 2000; Lewis et al. 1998; Twyman and Macdonald 1991). The biexponential current decay of macroscopic

GlyR channel currents after the end of glycine pulses may parallel the finding of different open states on the single channel level. As reported by Jones and Westbrook (1995) for GABA_A receptor channels and adopted by Harty and Manis (1998) for native GlyR channels, our results support the idea that desensitization in the prolonged presence of glycine may account for the prolongation of the deactivation. 4. Resensitization is a measure for the speed of transition from desensitized receptor states with bound ligands to activatable states. In contrast to experiments on native GlyR channels (Harty and Manis 1998), resensitization of recombinant GlyR channels could be fitted with a single exponential which increased with increasing pulse duration. There was no difference between α_1 -GlyR and $\alpha_1\beta$ -GlyR channels (Fig. 6).

For a detailed quantitative analysis, the kinetic data for activation, desensitization, deactivation, and resensitization must be integrated with the single channel data demonstrating different open states of the GlyR channels. The macroscopic GlyR channel currents share some properties with recombinant $\alpha_1\beta_3\gamma_2\text{L}$ GABA_A receptor channel currents in the study of Haas and Macdonald (1999). The authors report a computer simulation of the activation, deactivation, and desensitization kinetics of these channels by a linear model with three open and three desensitized states. In the next step, we shall adopt this model for a quantitative analysis of recombinant GlyR channel currents. The quantitative analysis will give detailed knowledge of the kinetic behavior of GlyR channels and especially help to clarify the molecular mechanism of GlyR channels in pathological states such as hyperekplexia (Langosch et al. 1994; Lewis et al. 1998).

Acknowledgements We thank Prof. H. Betz, Frankfurt, for the kind gift of cDNAs of glycine receptors, U. Jensen for expert technical assistance, and A. Niesel and J. Kilian for technical support. This study was supported by grants from the Deutsche Forschungsgemeinschaft and the Medizinische Hochschule Hannover.

References

- Becker CM, Hoch W, Betz H (1988) Glycine receptor heterogeneity in rat spinal cord during postnatal development. *EMBO J* 7:3717–3726
- Betz H (1990) Ligand-gated ion channels in the brain: the amino acid receptor superfamily. *Neuron* 5:383–392
- Betz H, Kuhse J, Schmieden V, Malosio ML, Langosch D, Prior P, Schmitt B, Kirsch J (1991) How to build a glycinergic postsynaptic membrane. *J Cell Sci Suppl* 15:23–25
- Bormann J, Rundstrom N, Betz H, Langosch D (1993) Residues within transmembrane segment M2 determine chloride conductance of glycine receptor homo- and hetero-oligomers. *EMBO J* 12:3729–3737
- Bufler J, Franke C, Parnas H, Dudel J (1996) Open channel block by physostigmine and procaine in embryonic-like nicotinic receptors of mouse muscle. *Eur J Neurosci* 8:677–687
- Franke C, Hatt H, Dudel J (1987) Liquid filament switch for ultrafast exchanges of solutions at excised patches of synaptic membrane of crayfish muscle. *Neurosci Lett* 77:199–204
- Graham D, Pfeiffer F, Simler R, Betz H (1985) Purification and characterization of the glycine receptor of pig spinal cord. *Biochemistry* 24:990–994
- Grenningloh G, Schmieden V, Schofield PR, Seeburg PH, Siddique T, Mohandas TK, Becker CM, Betz H (1990) Alpha subunit variants of the human glycine receptor: primary structures, functional expression and chromosomal localization of the corresponding genes. *EMBO J* 9:771–776
- Grewer C (1999) Investigation of the alpha(1)-glycine receptor channel-opening kinetics in the submillisecond time domain. *Biophys J* 77:727–738
- Haas KF, Macdonald RL (1999) GABAA receptor subunit gamma2 and delta subtypes confer unique kinetic properties on recombinant GABAA receptor currents in mouse fibroblasts. *J Physiol* 514:27–45
- Hamill OP, Marty A, Neher E, Sakmann B, Sigworth FJ (1981) Improved patch-clamp techniques for high-resolution current recording from cells and cell-free membrane patches. *Pflügers Arch* 391:85–100
- Handford CA, Lynch JW, Baker E, Webb GC, Ford JH, Sutherland GR, Schofield PR (1996) The human glycine receptor beta subunit: primary structure, functional characterisation and chromosomal localisation of the human and murine genes. *Brain Res Mol Brain Res* 35:211–219
- Harty TP, Manis PB (1998) Kinetic analysis of glycine receptor currents in ventral cochlear nucleus. *J Neurophysiol* 79:1891–1901.
- Jahn K, Bufler J, Franke C (1998) Kinetics of AMPA-type glutamate receptor channels in rat caudate-putamen neurones show a wide range of desensitization but distinct recovery characteristics. *Eur J Neurosci* 10:664–672
- Jahn K, Mohammadi B, Krampfl K, Abicht A, Lochmuller H, Bufler J (2001) Deactivation and desensitization of mouse embryonic- and adult-type nicotinic receptor channel currents. *Neurosci Lett* 307:89–92
- Jones MV, Westbrook GL (1995) Desensitized states prolong GABAA channel responses to brief agonist pulses. *Neuron* 15:181–191
- Kandel ER, Schwartz JH, Jesell TM (1995) *Essentials of neural science and behaviour*. Appleton & Lange, Stanford, Conn.
- Krampfl K, Bufler J, Lepier A, Dudel J, Adelsberger H (2000) Desensitization characteristics of rat recombinant GABA(A) receptors consisting of alpha1beta2gamma2S and alpha1beta2 subunits expressed in HEK293 cells. *Neurosci Lett* 278:21–24
- Krampfl K, Schlesinger F, Zorner A, Kappler M, Dengler R, Bufler J (2002a) Control of kinetic properties of GluR2 flop AMPA-type channels: impact of R/G nuclear editing. *Eur J Neurosci* 15:51–62
- Krampfl K, Wolfes H, Dengler R, Bufler J (2002b) Kinetic analysis of the agonistic and blocking properties of pentobarbital on recombinant rat alpha(1)beta(2)gamma(2S) GABA(A) receptor channels. *Eur J Pharmacol* 435:1–8
- Kuhse J, Schmieden V, Betz H (1990) A single amino acid exchange alters the pharmacology of neonatal rat glycine receptor subunit. *Neuron* 5:867–873
- Kuhse J, Kuryatov A, Maulet Y, Malosio ML, Schmieden V, Betz H (1991) Alternative splicing generates two isoforms of the alpha 2 subunit of the inhibitory glycine receptor. *FEBS Lett* 283:73–77
- Langosch D, Becker CM, Betz H (1990) The inhibitory glycine receptor: a ligand-gated chloride channel of the central nervous system. *Eur J Biochem* 194:1–8
- Langosch D, Laube B, Rundstrom N, Schmieden V, Bormann J, Betz H (1994) Decreased agonist affinity and chloride conductance of mutant glycine receptors associated with human hereditary hyperekplexia. *EMBO J* 13:4223–4228
- Laube B, Kuhse J, Betz H (2000) Kinetic and mutational analysis of Zn2+ modulation of recombinant human inhibitory glycine receptors. *J Physiol* 577:215–230
- Legendre P (1997) Pharmacological evidence for two types of postsynaptic glycinergic receptors on the Mauthner cell of 52-h-old zebrafish larvae. *J Neurophysiol* 77:2400–2415
- Legendre P (1998) A reluctant gating mode of glycine receptor channels determines the time course of inhibitory miniature synaptic events in zebrafish hindbrain neurons. *J Neurosci* 18:2856–2870
- Lewis TM, Sivilotti LG, Colquhoun D, Gardiner RM, Schoepfer R, Rees M (1998) Properties of human glycine receptors containing the hyperekplexia mutation alpha1(K276E), expressed in *Xenopus oocytes*. *J Physiol* 507:25–40
- Malosio ML, Marqueze-Pouey B, Kuhse J, Betz H (1991) Widespread expression of glycine receptor subunit mRNAs in the adult and developing rat brain. *EMBO J* 10:2401–2409
- Mohammadi B, Krampfl K, Moschref H, Dengler R, Bufler J (2001) Interaction of the neuroprotective drug riluzole with GABA(A) and glycine receptor channels. *Eur J Pharmacol* 415:135–140
- Rajendra S, Lynch JW, Pierce KD, French CR, Barry PH, Schofield PR (1995) Mutation of an arginine residue in the human glycine receptor transforms beta-alanine and taurine from agonists into competitive antagonists. *Neuron* 14:169–175
- Schmieden V, Grenningloh G, Schofield PR, Betz H (1989) Functional expression in *Xenopus oocytes* of the strychnine binding 48 kd subunit of the glycine receptor. *EMBO J* 8:695–700
- Schmieden V, Kuhse J, Betz H (1992) Agonist pharmacology of neonatal and adult glycine receptor alpha subunits: identification of amino acid residues involved in taurine activation. *EMBO J* 11:2025–2032
- Singer JH, Berger AJ (1999) Contribution of single-channel properties to the time course and amplitude variance of quantal glycine currents recorded in rat motoneurons. *J Neurophysiol* 81:1608–1616.
- Twyman RE, Macdonald RL (1991) Kinetic properties of the glycine receptor main- and sub-conductance states of mouse spinal cord neurones in culture. *J Physiol* 435:303–331
- Unwin N (1989) The structure of ion channels in membranes of excitable cells. *Neuron* 3:665–676
- Watanabe E, Akagi H (1995) Distribution patterns of mRNAs encoding glycine receptor channels in the developing rat spinal cord. *Neurosci Res* 23:377–382
- Wyllie DJA, Béhé P, Colquhoun D (1998) Single-channel activation and concentration jumps: comparison of recombinant NR1a/NR2A and NR1a/NR2D NMDA receptors. *J Physiol* 610:1–18